RSC Advances

This article can be cited before page numbers have been issued, to do this please use: D. Giri and S. K. Patra, *RSC Adv.*, 2015, DOI: 10.1039/C5RA14079J.

ROYAL SOCIETY
OF CHEMISTRY

www.rsc.org/advances

View Article Online
DOI: 10.1039/C5RA14079J

Journal Name

ARTICLE

Benzodithieno-imidazole based π-conjugated fluorescent polymer probe for selective sensing of Cu^{2+}

Received 00th January 20xx,
Accepted 00th January 20xx

DOI: 10.1039/x0xx00000x

www.rsc.org/

Dipanjan Giri[a], and Sanjib K Patra[a]*

The π-conjugated polymers appended with binding sites, is of considerable interest as evolving new class of heavy and toxic metal-ion sensors through fluorescence quenching. In this study we describe the synthesis and characterization of *p*-bromophenyl substituted benzodithieno-imidazole based soluble and rigid π-conjugated polymer with N and S donors exhibiting outstanding sensitivity towards Cu^{2+} by emission quenching through photoinduced electron transfer (PET). The detailed photophysical and ion sensing studies have been demosntrated to understand the insight of polymer-metal ion interaction which is responsible for selective fluorescence quenching. The corresponding polymer is also explored as thin-film polymeric sensor towards Cu^{2+}as monitored by photoluminescence study.

Introduction

The development of highly sensitive and selective chemosensory materials for the detection of metal ions in environmental or biological systems has gained remarkable interest in the recent years.[1] Since heavy metal ions are significant pollutants and many of them are essential trace elements in biological systems, various fluorescent sensors of heavy metal ions have been developed for selective detection.[2] For the detection of transition metal ions, binding sites are generated through the modification of the coordination sites through judicious design and synthesis.[3]

Copper is the third most abundant transition metal ions found in all living organisms and is an essential trace element in redox chemistry. Several enzymes and proteins involved in metabolism, respiration, and DNA synthesis, such as cytochrome oxidase, superoxide dismutase, ascorbate oxidase, and tyrosinase go through the copper cycle. The imbalance of copper in living body results various diseases such as Wilson disease (WD),[4] Alzheimer's disease,[5] Haematological manifestation and Menkes disease (MD).[6] Therefore a reliable easy method for the detection of trace amount of copper ion in biological and environmental samples is essential.

Many advanced methods such as spectrophotometry, atomic absorption spectroscopy, inductively coupled plasma mass spectroscopy, conductometric detection have been developed for qualitative and quantitative detection of Cu^{2+} ion.[7] Among them, due to the excellent sensitivity as well as selectivity, non-destructiveness, and economic nature, the fluorescence technique is the mostly used and rapidly expanding method in the field of the chemical sensing.[8] This process offers highly sensitive optical transduction method for analyte-binding events, which are based upon changes in intensity, energy transfer, wavelength shift (excitation and emission), optical changes and lifetime. The intramolecular charge transfer (ICT) and photo-induced electron transfer (PET) fluorescence mechanisms have been exploited to demonstrate the turn-on or turn-off fluorescence response during the sensing event by fluorescence sensors. In recent years many probes such as cyclen, imidazoquinoxaline, imidazopyrene, imidazophenazine, rhodamine, calixarene, bis(N-methylndolyl)methane, triazole based dansyl, dipicolylamine, 2,2'-dipicolylamine,N,N,N',N'-tetrakis(2-pyridylmethyl)ethylenediamine based fluorescence sensors for heavy metal ions such as Zn^{2+}, Pb^{2+}, Hg^{2+}, Cd^{2+}, and Cu^{2+} are successfully designed and developed with small molecule fluorophores as well as polymer probes by various groups.[9]

The field of π-conjugated polymer-based metal ion sensor is of considerable interest and is rapidly developing research interest with well defined systems via fluorescence quenching mechanism. Thus the desired polymer regime can be integrated with the incorporation of main-chain or side-chain with strong binding sites. The delocalized π-electronic conjugated polymer exhibits a prominent candidate for sensitivity enhancement in fluorescence quenching process due to the fast and facile energy migration along the π-conjugated chain, resulting in optical signals for transduction of chemical or biological events as demonstrated by various groups.[10] In spite of wide research in this field, it remain largely unknown, how the structural modification on the coordination site and the substituent helps the sensing efficacy. We are interested in investigating the structural modification of the fluorophores through the rational design of

---

[a] *Department of Chemistry, Indian Institute of Technology Kharagpur, Kharagpur-721302, WB, INDIA, E-mail: skpatra@chem.iitkgp.ernet.in; Tel: +913222283338*

† Electronic Supplementary Information (ESI) available: [Full experimental details and characterization data, full photophysical and sensing studies, and X-ray crystallographic data]. See DOI: 10.1039/x0xx00000x

View Article Online
DOI: 10.1039/C5RA14079J

molecular architectures searching for an efficient polymer probe for metal ions. In this work, we report benzothieno-imidazole based π-conjugated luminescent polymeric probes having nitrogen and sulphur donor acting as chelating sites for selective sensing of metal ions. Lin and co-workers first showed that the benzothieno-imidazole moiety can be used as a good sensory probe for toxic heavy metal cations.[11] Furthermore the presence of both hard "N" and soft "S" donors could be an efficient fluorescent sensor for selective transition metal cations having border line acidic nature such as Cu^{2+}. The corresponding polymer is also investigated for sensory applications towards Cu^{2+} as thin film polymeric sensor as monitored by photoluminescence (PL) study.

Results and Discussion

Synthesis and Characterization

A good chelating or a binding site is necessary to improve the binding constant and as well as enhancing the fluorescence response.[12] For this reason the benzodithieno-imidazole based ligand containing the two donor hetero atoms, nitrogen and sulphur, first introduced by Lin and co-workers[11] have been explored in this work. The key precursor of this work, 3,3'-bithiophene (**1**) was synthesized from 3-bromothiophene by treating with *n*-BuLi at -78°C followed by anhydrous $CuCl_2$ at -50°C in diethyl ether, through Gilman coupling. The resulting white solid was purified through column chromatography using hexane as eluent to get **1** in 76% yield. The ^1H NMR shows two multiplets, one at 7.37-7.38 ppm for the two protons adjacent to sulphur (5 and 5'-position) atom and another multiplet at 7.36-7.33 ppm for the remaining four thienyl protons. Acylation of **1** by oxalyl chloride in 1,2-DCE at 95°C yielded **2** as shiny reddish solid with 64% yield. In ^1H NMR the signal at 7.83 ppm signifies two more deshielded protons adjacent to sulphur atom, and the resonance at 7.29 ppm is attributed to the other two less deshielded protons. Compound **2** was coupled with 4-substituted benzaldehydes (4-methyl benzaldehyde and 4-bromo benzaldehyde) as shown in Scheme 1, in the presence of ammonium acetate in acetic acid medium to get the compound **3a** and **3b** respectively as greenish solid. As these compounds are insoluble in common organic solvent, alkylation is necessary to improve the solubility. For this N-alkylation was performed by treating with potassium carbonate and *n*-iodoheptane. The compound was purified through column chromatography using EtOAc-Hexane (4:1) as eluent to obtain the analytically pure yellow solid of **4a** (*p*-tolylbenzodithieno-imidazole) and **4b** (*p*-bromophenylbenzodithieno-imidazole) in 55% and 53% yield respectively. The formation of **4a** was confirmed by ^1H NMR spectrum in $CDCl_3$, showing two doublets at 7.67 ppm and 7.36 ppm corresponding to four thiophene protons. The two benzene protons (ortho to Me) resonate as triplet centred at 7.52 ppm whether other two protons resonate as doublet of doublets at 7.80 and 7.87 ppm. The methyl protons appear at 2.46 ppm as singlet. The characteristics peak at 4.51 ppm represents the two methylene protons attached to N atom. For **4b** signals at 7.83 ppm and 7.60 ppm signify the four thiophene proton, whereas four benzene protons resonate at 7.73 ppm as multiplet and at 7.51 ppm as doublet. HRMS (ESI^+) study also confirms the formation of product **4a** and **4b** by showing the molecular ion peak at 419.1599 ($[M+H]^+$)and 483.3438 ($[M+H]^+$) respectively. For **4b** the yellow needle-like single crystals suitable for X-ray crystallography were harvested by layering THF solution of **4b** on water. The **4b** crystallizes in triclinic system with space group $P\bar{1}$. The crystal structure of **4b** consists of two independent molecules in an asymmetric unit with negligible differences in metrical parameters. The molecular structure (ORTEP representation) of one of the molecule in the asymmetric unit is shown in Fig. 1. The X-ray study reveals the planar conformation of the benzodithieneo-imodazole core confirming higher degree of π-electron delocalization which is also reflected in the photophysical properties of the **4b** and the corresponding π-conjugated rigid polymer, **P2** (*vide infra*). The phenyl and the benzodithieno-imidazole rings are nearly orthogonal to each other as manifested by the torsion angle (C5-C4-C7-N1) of 83.8°.

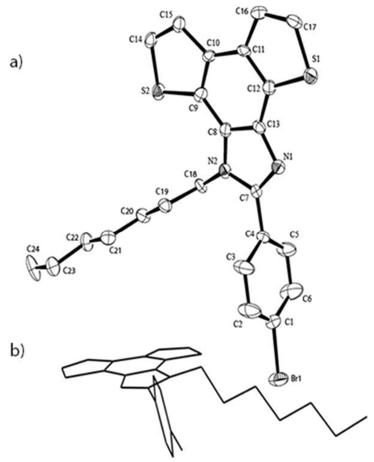

Fig. 1 a) ORTEP representation **4b** with atoms labelled. The thermal ellipsoids are drawn at 40% of probability. b) Side view as stick model. Hydrogen atoms have been omitted for sake of clarity.

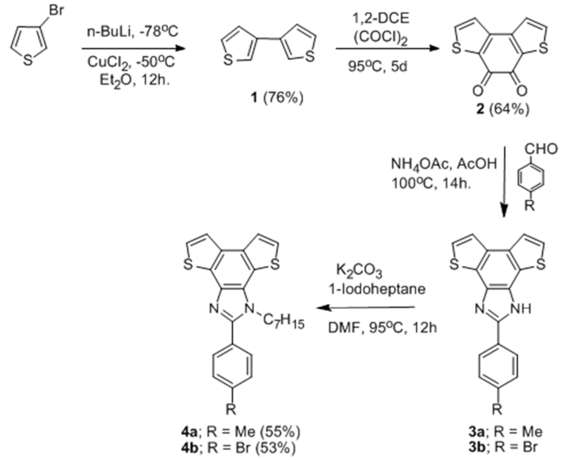

Scheme 1 Synthetic route for **4a** and **4b** (yield in parenthesis).

View Article Online
DOI: 10.1039/C5RA14079J

To access the corresponding polymers of **4a** and **4b** through step growth polymerization, the respective monomers **5a** and **5b** were prepared through bromination using N-bromosuccinamide (NBS) in 80-85% yield.[11a] However Grignard Reagent Metathesis (GRIM)[13] was unsuccessful in the presence of Ni(dppp)Cl_2 (dppp = 1,3-bis(diphenylphosphino)propane) in combination with the various Grignard reagents such as *t*-BuMgCl, *i*-PrMgBr, cyclohexylMgBr and turbo Grignard (*i*-PrMgCl.LiCl) reagents in various reaction condition (see Table S2†). Stille polymerization protocol of **5a** and **5b** was followed to obtain the corresponding π-conjugated polymers as shown in Scheme 2. Addition of *n*-butyllithium followed by tributyltinchloride at -78°C to **5a** and **5b** afforded the respective bis(tributylstannyl) derivatives **6a** and **6b**, which were used directly for Stille polymerization.[14] Polymerization was performed with **5a** and **6a** in the presence of $Pd(PPh_3)_4$ catalyst through Stille polymerization protocol[15] to get **P1** (Scheme 2). In a similar strategy **P2** was also synthesized. The polymers were isolated through precipitation in methanol. The polymer was further purified through Soxhlet extractor by using hexane, then MeOH, and finally the polymer was extracted with DCM. Then DCM solution was concentrated and precipitated in stirring distilled hexane. The precipitate was washed four times with hexane to get the desired brownish colored polymer. The polymerization condition and characterization data are shown in Table 1. The polymers were found to be readily soluble in common organic solvents and exhibit a strong cyan fluorescence. The luminescent π-conjugated polymers were characterized by various spectroscopic tools. The disappearance of the alkyl protons of 'SnBu$_3$' in ^{1}H NMR and disappearance of the signal at 112.2 and 111.5 ppm in ^{13}C NMR corresponding to thienyl carbons attached to 'Br' reveal polymerization of **5b** and **6b**. The formation of the polymer was further confirmed by Tetradetector Gel Permeation Charomatography (GPC) as shown in Fig. 2. The molecular weight distribution with PDI of 1.81 and 1.67 was observed for **P1** and **P2** respectively indicating the step-growth polymerization of the corresponding monomers.

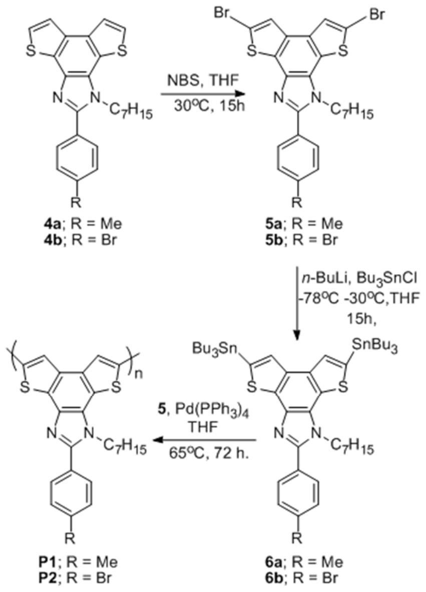

Scheme 2 Synthetic route for the polymers **P1** and **P2** from **4a** and **4b** respectively.

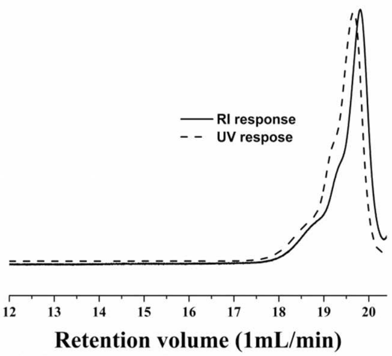

Fig. 2 GPC trace (Refractive Index and UV responses) of **P2** using THF as eluent. PDI (M_w/M_n) of **P2** was found to be 1.67.

Table 1 Characterization of the polymers synthesized through Stille polymerization.[a]

Polymer	Yield	Mn, Da	PDI (Mw/Mn)
P1	65%	14,799	1.81
P2	68%	15,519	1.67

[a] Stille polymerization of **5a** and **5b** in THF was carried out at 65°C for 72 h using $Pd(PPh_3)_4$ as catalyst (5 mol%).

Photophysical studies

The absorption studies of **4a** and **4b** in DMSO show two absorption maxima, one at high energy centred at 270 nm and the second one with low energy in the range of 320-350 nm.

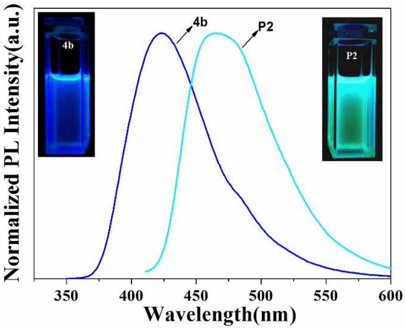

Fig. 3 Emission spectra of **4b** and **P2** (~2 x 10^{-5} M) in DMSO:H_2O (1:1), excited at 340 and 400 nm respectively. Inset: Visible color changes of **4b** (left) and **P2** (right) under UV illumination at 365 nm.

The low energy absorption bands (333 nm for **4a** and 340 nm for **4b**) are assigned to π-π* transition involving the molecular orbital of benzodithieno and imidazole moeity. The florescence response of the fluorophore **4a** and **4b** was explored in DMSO (Fig. S36†) exhibiting strong blue fluorescence centred at 407 (λ_{exct} = 333 nm) and 422 nm (λ_{exct} = 340 nm) respectively. The low energy absorption for both the polymers are red shifted by 55-60 nm compared to that of the corresponding monomers,

DOI: 10.1039/C5RA14079J

suggesting extensive π-delocalization through the polymer backbone (Fig. S51†). The florescence response of **P1** and **P2** was investigated (in DMSO:H_2O) showing cyan emission centred at 460 nm and 468 nm respectively which were again 40-60 nm red shifted from the blue emissive **4a** and **4b** as shown in Fig. 3. The quantum yield (ϕ_f) of emission of **4a**, **4b** and the corresponding polymers **P1** and **P2** in DMSO:H_2O (1:1) was 0.19, 0.09, 0.21 and 0.23 respectively (Table 2) with reference to quinine sulphate in 0.1 M H_2SO_4 solution which was calculated according the literature procedure as described in ESI†.

Table 2 Absorption and fluorescence properties of **4a, 4b, P1** and **P2** in DMSO:H_2O (1:1).

Fluorophore	Absorbance		Luminescence		
	λ_{max} (nm)	ε (L.mol^{-1}.cm^{-1}) × 10^2	λ_{exct} (nm)	λ_{em} (nm)	Φ_f^*
4a	308, 333	198, 71	333	407	0.19
4b	270, 340	196, 78	340	422	0.09
P1	279, 395	273, 226	395	460	0.21
P2	279, 400	298, 185	400	468	0.23

*Quinine sulphate in 0.1 M H_2SO_4 was used as reference for quantum yield calculation with Φ_f = 0.57.

Metal ion sensing properties:

Before studying metal ion complexation of polymers for demonstrating sensory property towards transition metal cations, we investigated the metal coordination with the corresponding monomers searching for an efficient and selective sensor for Cu^{2+}. After the complete characterization sensing ability of **4a** and **4b** fluorophores were verified with different metal cations. Thus the absorbance and fluorescence response of **4a** and **4b** for different metal ions such as Co^{2+}, Cu^{2+}, Ni^{2+}, Zn^{2+}, Cd^{2+}, Pb^{2+}, Cr^{3+}, Fe^{3+}, Hg^{2+}, Ba^{2+} and Sr^{2+} were investigated in DMSO:H_2O to examine the selective response to Cu^{2+}. The fluorophore and the metal ions were dissolved in DMSO and water respectively. The solution of these metal cations were prepared in water in ~1 x 10^{-5} M concentration and were added to the stock solution of **4a** and **4b** which was also prepared in ~1 x 10^{-5} M concentration in DMSO by maintaining the 1:1 metal ligand ratio. The fluorophore **4a** with the electron donating 'Me' substituted congener does not show any significant change in absorption or in PL intensity upon addition of different metal cations (Fig. S37† and S38†). Interestingly **4b** with electron withdrawing 'Br' substituent shows a significant photophysical change upon addition of Cu^{2+} ion indicating the preferential selectivity towards Cu^{2+} among various competing metal cations. Considering the absorption spectrum of **4b** as shown in Fig. S39†, the absorption maxima of the free ligand was observed at 270 nm and 340 nm. The absorption was due to the π-π* transition involving the imidazole and dithieno moiety. On addition of different metal ions the absorption maxima blue shifted by *ca.* 10 nm compared to the absorption of the free ligand. Surprisingly after addition of Cu^{2+} the absorption maximum at 340 nm (corresponding transition) to π to π* was diminished and a new absorption maximum at 286 nm appeared, indicating the coordination of Cu^{2+} to the binding sites of **4b**. The absorption study clearly shows that the fluorophore **4b** can selectively bind to Cu^{2+}, which is further demonstrated by fluorescence quenching after coordination to paramagnetic Cu^{2+} selectively as demonstrated in Fig. 4.

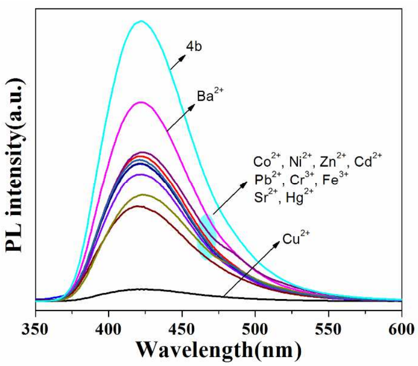

Fig. 4 Emission spectra of **4b** (~ 2 x 10^{-5} M) in presence of different metal ion in DMSO:H_2O (1:1).

To study the sensing in more depth and to ensure the phenomenon, a titration of ligand **4b** with Cu^{2+} solution was performed with increasing concentrations of Cu^{2+} and the UV-Vis absorption (Fig. S43†) as well as emission (Fig. S44†) spectral responses were recorded. The absorption maxima at 340 nm corresponding to the free ligand decreases upon increasing the concentration of Cu^{2+}, probably due to the gradual diminishing of the π-π* transition from imidazole to benzodithieno as a result of the adduct formation with Cu^{2+}. The isosbestic point at 327 nm revealed the existence of a single equilibrium between the free ligand and the Cu^{2+} bound ligand. The emission spectrum shows a gradual quenching upon increasing the Cu^{2+} concentration and at higher concentration (2 x 10^{-4} M) of Cu^{2+} the fluorescence completely quenched. Saturation of PL intensity was observed on addition of 0.6 eqv of Cu^{2+} suggesting 2:1 (**4b.**Cu^{2+}) stoichiometry. This was further confirmed by continuous variation method (Job's plot) as depicted in Fig. 5. The intensity at 422 nm was plotted

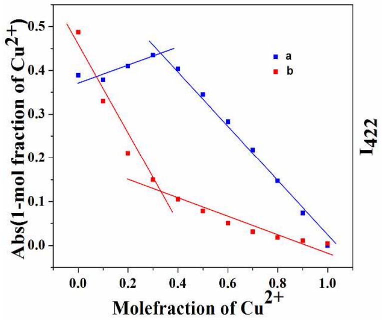

Fig. 5 Job's plot showing 2:1 binding stoichiomtery between **4b** and Cu^{2+} in DMSO:H_2O, Plot recorded from a)absorbance titration, b) emission titration.

View Article Online
DOI: 10.1039/C5RA14079J

against the mole fraction of Cu^{2+} at a constant total concentration ($[Cu^{2+}]$.**4b**) of 20 mM and spectra were acquired in DMSO:H_2O(1:1). The association constant of Cu^{2+} with **4b** was found to be 5.2(±0.2) × 10^4 indicating thermodynamically stable binding between the border line Cu^{2+} and the **4b** ligand containing N, S donors, which can be studied by Stern-Volmer[10a,16] equation ($F_0/F = (1+ K_{SV}[Q])$) (Fig. S45†). The **4b**.Cu^{2+} metal complex was isolated by reacting **4b** and $Cu(NO_3)_2$ in THF-methanol mixture. The MALDI-TOF study confirms 2:1 **4b.**Cu^{2+} complex by showing molecular ion peak at 1029.700 as observed by photophysical studies. The isotopic mass distribution of the complex (**4b.**Cu^{2+}) with the proposed structure of the metal complex is shown in Fig. 6.

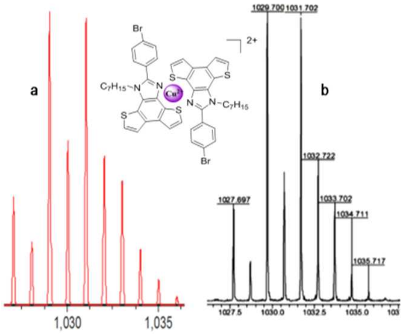

Fig. 6 a) Simulated and b) Experimental isotopic distribution of $(\mathbf{4b})_2.Cu^{2+}$, with the proposed schematic representation of the binding sites where Cu^{2+} metal ion are bound to the **4b.**

One of the most important criteria for a selective cation probe is the ability to sense of a particular cation in presence of other competitive and similar cations. To show the selectivity towards Cu^{2+}, florescence intensity measurement of **P2** was carried out in the presence of Cu^{2+} ions mixed with other metal cations such as Co^{2+}, Ni^{2+}, Zn^{2+}, Cd^{2+}, Pb^{2+}, Cr^{3+}, Fe^{3+}, Hg^{2+}, Ba^{2+} and Sr^{2+}. It was observed having excellent selectivity towards Cu^{2+} without showing any interference in the vicinity of other metal cations as shown in Fig. 7.

After the successful sensing study of **4b** towards the Cu^{2+} selectively, we were encouraged to explore the corresponding π-conjugated polymer as probe for Cu^{2+} aiming for thin film metal ion sensing. The polymer **P2** also shows selective sensing towards Cu^{2+} as observed for the monomer as monitored by quenching in emission in the presence of Cu^{2+}. The selectivity towards the Cu^{2+} in presence of other ions (Fig. 8) of the polymer was performed, which again shows the polymer can be used as a selective Cu^{2+} sensor. The visually noticeable fluorescence quenching in naked eye (under UV illumination at 365 nm) makes **P2** an efficient sensor for Cu^{2+} as demonstrated in Fig. 9. The absorption and fluorescence titration by varying the amount of Cu^{2+} was also performed showing significant change in photophysical properties. The solution of these metal salts were prepared in DMSO:H_2O (1:1) in ~2 x 10^{-5} M concentration and were added to the stock solution of polymer **P2**. The similar protocol for the absorption and emission titration was followed as performed for the case of **4b**. From the titration profile it is obvious that the absorption maxima at 400 nm (Fig. 10) of polymer decreases while λ_{max} at 279 nm increases with increasing the concentration of Cu^{2+} accompanied by an isosbestic point at 348 nm suggesting a single equilibrium between the free polymer and Cu^{2+}-coordinated metallopolymer. Gradual quenching in emission with increasing the concentration of Cu^{2+} (Fig. 11) was observed as expected. However the complete quenching of fluorescence of the polymer backbone was not observed by the ligand-metal ion interaction unlike the monomer where complete quenching of fluorescence was observed, presumably due to the unavailability of all the coordination sites to metal ions in the polymer backbone.[12a,17] It is noteworthy to mention that the limit of detection of **P2** and **4b** for Cu^{2+} (5.29 x 10^{-7} M^{-1} and 6.53 x 10^{-7} M^{-1} respectively) is sufficiently below than the limit of copper in drinking water (20 μM) as calculated from the concentration dependent

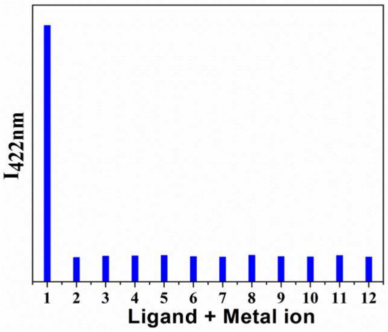

Fig. 7 Metal specificity of **4b** in DMSO:H_2O with a mixture of Cu^{2+} and other metal ions (~2 x 10^{-5} M). 1-12 represent (1) free **4b**; (2) **4b** + Ba^{2+}; (3) **4b** + Sr^{2+}; (4) **4b** + Cd^{2+}; (5) **4b** + Co^{2+}; (6) **4b** + Fe^{3+}; (7) **4b** + Zn^{2+}; (8) **4b** + Cr^{3+}; (9) **4b** + Ni^{2+}; (10) **4b** + Pb^{2+}; (11) **4b** + Hg^{2+}; (12) **4b** + all

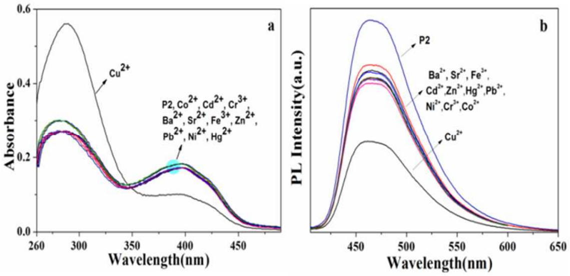

Fig. 8 a) Absorbance spectra of **P2** (~2 x 10^{-5} M) in presence of different metal ion in DMSO:H_2O (1:1). (b) Emission spectra of **P2** (~2 x 10^{-5} M) in presence of different metal ion in DMSO:H_2O (1:1).

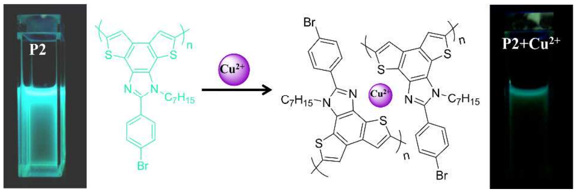

Fig. 9 Visual changes observed in emission of free **P2** (left) and Cu^{2+}-coordinated **P2.**Cu^{2+} (right) under UV illumination at 365 nm.

View Article Online
DOI: 10.1039/C5RA14079J

fluorescence studies shown in Fig. S52†.

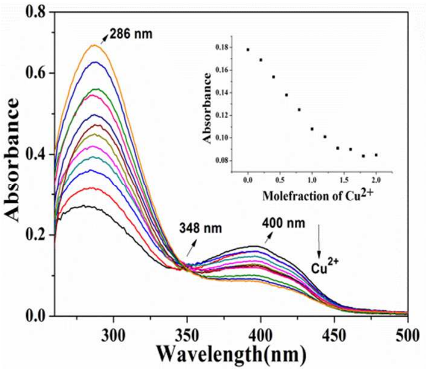

Fig. 10 Absorbance spectra of **P2** (~2x 10^{-5}) in DMSO:H_2O (1:1) in the presence of different equivalent of Cu^{2+}.

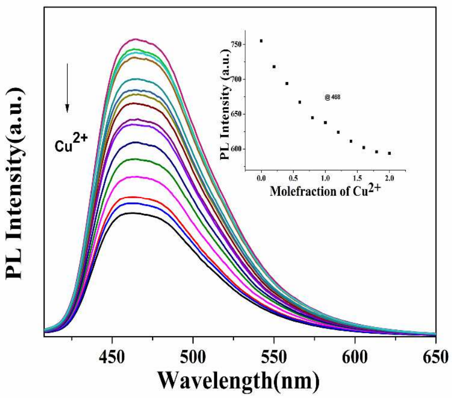

Fig. 11 Emission spectra of **P2** (~2 x 10^{-5} M) in presence of different metal ion in DMSO:H_2O (1:1).

Table 3 Fluorescence life time measurements of **4b** and **P2** upon the addition of Cu^{2+} in DMSO:H_2O (1:1)

	λ_{em}(nm)	$\langle\tau\rangle^a$ (ns)
4b	400	1.88
4b.Cu^{2+}	400	1.64
P2	468	2.83^b
P2.Cu^{2+}	468	2.34^c

[a] Error in experimental data ±5%

[b] τ_1(ns)=2.55, α_1=0.67, τ_2(ns)=3.43, α_2=0.33

[c] τ_1(ns)=2.05, α_1=0.79, τ_2(ns)=3.25, α_2=0.21

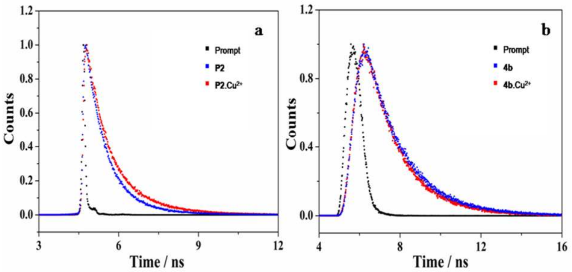

Fig. 12 a) Fluorescence life time decay of **4b** and **4b.**Cu^{2+} system, (b) Fluorescence life time decay of **P2** and **P2.**Cu^{2+} system.

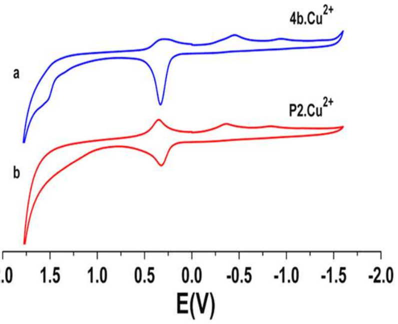

Fig. 13 Cyclic voltammogram studies of (a) **4b**.$Cu^{2+}$and (b) **P2**.Cu^{2+} in DMF using 0.1 M $TBAPF_6$ as supporting electrolyte, Pt disc working electrode and Ag/AgCl reference electrode. Scan rate at 100 mV/s.

Thus after coordination to paramagnetic Cu^{2+} ion, emission at 468 nm of **P2** was quenched which was not observed in case of other competing metal cations. Probably the soft and hard binding sites associated with sulphur and nitrogen atoms can bind preferentially to the border line acid Cu^{2+}. The emission quenching phenomena is generally observed from the three major mechanism of fluorescence transduction such as intra molecular charge transfer (ICT),[18] fluorescence resonance energy transfer (FRET),[19] and photoinduced electron transfer (PET).[1e,20] FRET is ruled out considering the negligible overlap region between the absorption and emission of the fluorophore unit. The absence of separate interacting and proximal donor-acceptor pair in this system further excludes the possibility of FRET. ICT is also unlikely as there is no possibility of formation of ICT structure in this probe. The emission quenching of **4b** and the π-conjugated polymer (**P2**) after Cu^{2+} coordination is mainly due to the photoinduced electron transfer interaction between the fluorophore unit and paramagnetic Cu^{2+} as reported in previous literature.[21] In our case, upon binding the ligand with Cu^{2+} there is a large quenching of fluorescence intensity as reflected by the very low quantum yield (ϕ=0.002). We propose that the chelating site with "N" and "S" heteroatoms are responsible for binding with metal cations. However **4a** and **P1** did not show any change in PL intensity after addition of Cu^{2+} (*vide supra*). To understand the different photophysical response of **4a** and **4b** towards Cu^{2+} we calculated HOMO and LUMO of the fluorophores by electrochemical studies (ESI†). Presumably the d_{x2-y2} orbital accommodating the unpaired electron of paramagnetic Cu^{2+} (elongated octahedron) lies between the HOMO and LUMO of **4b**. The successful recognition of Cu^{2+} by **4b** through the possible PET mechanism has been demonstrated in Fig S54a† showing favourable energy difference between the LUMO (of **4b**) and d_{x2-y2} (of Cu^{2+}) leading to non-radiative deactivation of the excited state resulting of PL quenching.[21,22] The LUMO of **4a** (-3.02 eV) is significantly lower in energy than that of **4b** (-2.71 eV), and also presumably lower in energy than the d_{x2-y2} orbital. Hence the electron transfer is not facile from LUMO of **4a** to d_{x2-y2} of Cu^{2+} (Fig S54b†). The proposed phenomenon was further

View Article Online
DOI: 10.1039/C5RA14079J

supported by the fluorescence decay study (Fig. 12) by the Time-Correlated Single Photon Counting (TCSPC). In the fluorescence lifetime decay experiment (λ_{em} = 400 nm), the life time of free **4b** was found to be 1.88 ns whereas for **4b**.Cu^2 the life time was decreased to 1.64 ns. For **P2** (λ_{em} = 468 nm) the first life time component (τ_1) was 2.55 (67%) with a second component of 3.43 ns (33%), and an average life time (τ) of 2.83 ns**.** The average fluorescence life time of the corresponding Cu^{2+}-coordinated metal-containing polymer (**P2**.Cu^{2+}) decreased to 2.34 ns (Table 3) ascribing the collisional fluorescence quenching phenomenon.[23]

The Cu^{2+} coordinated complex **4b**, [Cu(**4b**)$_2$](NO$_3$)$_2$ and the corresponding metallopolymer (**P2.**Cu^{2+}) were also characterized by cyclic voltammetry study (Fig. 13). While recording CV at the window of +1.50 V to -1.50 V in DMF with scan rate of 100 mV/s two reduction peaks at -0.446 V and -0.943 V attributing to Cu^{2+}/Cu^{1+} and Cu^{1+}/Cu^0 reduction process were observed. The significantly intense anodic peak at +0.328 V is due to the deposition of Cu metal at the electrode surface as result Cu^{1+}/Cu^0 reduction.[3h,24] Similar behaviour was also observed for Cu^{2+} coordinated metallopolymer where less intense anodic peak at +0.318 V was observed presumably due to less amount of Cu deposition at the electrode surface in the presence of polymers.

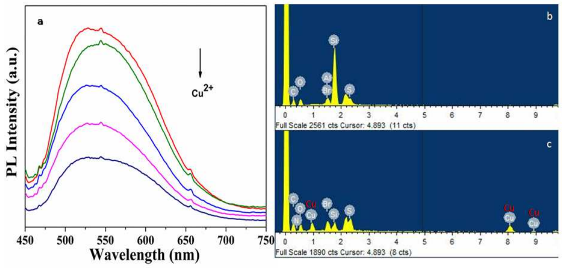

Fig. 14 a) Solid state PL spectra of **P2** thin film (on quartz plate) dipped for 15 min in different concentration of Cu^{2+} solution with. (~ 1 x 10^{-2} M, ~ 1 x 10^{-3} M, ~ 1 x 10^{-4} M, ~ 1 x 10^{-5} M). EDX analysis of b) **P2** polymer film coated on quartz plate c) Cu^{2+}-coordinated **P2**. Silicon is from the quartz substrate.

To demonstrate the practical application as on-site detection of Cu^{2+} by the polymer, we explored the detection by making polymeric film on quartz plate. Thin film of the polymer was prepared by spin coating on quartz plate, which was then immersed to the various concentration of Cu^{2+} aqueous solution (1mM to 1µM) followed by repetitive and extensive washing with Milli-Q water to remove any unbound free Cu^{2+} ion. Solid state PL study of the Cu^{2+}-coordinated polymeric film was performed to demonstrate a significant amount of quenching of the emission centred at 525 nm (Fig. 14). Energy Dispersive X-ray (EDX) analysis shows the presence of Cu confirming the formation of Cu^{2+}-coordinated metallopolymer. We also performed the gradual quenching of the PL intensity with the increasing time of immersion of the polymeric film in Cu^{2+} solution (1µM). It was observed that upon instant dipping of the quartz plate in Cu^{2+} solution there is no such quenching. However if we allow for longer time with 15 minutes or more in Cu^{2+} solution, intensity of PL spectra started to decrease significantly as shown in Fig. S56†, demonstrating that the polymer can be explored as a thin film sensor for Cu^{2+} ion detection.

Conclusion

In conclusion, soluble benzodithieno-imidazole based π-conjugated rigid polymers, appended with N, S donors, were synthesized through Stille coupling searching for an efficient polymer probe for biological and environmentally relevant Cu^{2+}. It is observed that the sensing ability is highly dependent on substituent as revealed in this study. The electron withdrawing ‘Br’ substituted *p*-bromophenylbenzodithieno-imidazole succeeds over electron donating ‘Me’ substituted *p*-tolylbenzodithieno-imidazole congener towards Cu^{2+} ion sensing. Thus the synthesized π-conjugated polymer **P2** shows outstanding fluorescence sensor for the recognition of paramagnetic Cu^{2+} with high sensitivity and selectivity through fluorescence quenching via photoinduced electron transfer. Its fluorescence intensity decreases in a linear fashion with the concentration of the Cu^{2+}, demonstrating as a potential candidate for selective sensing of Cu^{2+} in the presence of the different metal ions. The detailed photophysical and ion sensing including electrochemical studies were demonstrated to understand the insight of the polymer-metal ion interaction. Furthermore metal ion sensing ability by polymeric film of **P2** is examined to demonstrate the practical application as on-site detection of Cu^{2+}. This work reveals a novel platform for the further development of soluble π-conjugated fluorescent polymer based probes by fine tuning of the electronic factor for sensing environmentally relevant metal ions.

Acknowledgement

Authors acknowledge the financial support from the DST-SERB, India through Fast Track scheme (SB/FT/CS-010/2012). Authors thank Prof. Nilmoni Sarkar’s group (Dept. of Chemistry, IIT Kharagpur) for providing TCSPC measurement facilities. SKP thanks IIT Kharagpur for funding the purchase of the electrochemical workstation and Multidetector GPC through SGIRG (IIT/SRIC/CHY/PBR/2014-15/44) and SGDRI (IIT/SRIC/CHY/NPA/2014-15/81) grants (Competitive Research Infrastructure Seed Grant) respectively. A doctoral fellowship from IIT Kharagpur (to D.G.) is gratefully acknowledged.

Experimental section

Materials and Instrumentation

All the air and moisture sensitive reactions and manipulations were carried out under an atmosphere of pre-purified N$_2$ or Ar by using standard Schlenk techniques. The glasswares were oven-dried (at 180°C) and cooled under vacuum. Tetrahydrofuran and diethyl ether were dried over Na/benzophenone. All chemicals were purchased from Aldrich unless otherwise noted. Ammonium acetate and all metal salts

View Article Online
DOI: 10.1039/C5RA14079J

were acquired from Merck. The benzaldehyde derivatives were purchased from Spectrochem. Silica gel (60–120 and 100–200 mesh) used for column chromatography, was purchased from Merck. $Pd(PPh_3)_4$ was synthesized following the literature method.[25]

^{1}H (600 MHz, 400 MHz and 200 MHz), ^{13}C{^{1}H} (150 MHz, 100 MHz and 50MHz) NMR spectra were obtained from Bruker Lambda spectrometer using $CDCl_3$ unless otherwise mentioned. Spectra were internally referenced to residual solvent peaks (δ = 7.26 ppm for proton and δ = 77.23 for carbon (middle peak) in $CDCl_3$). All coupling constants (*J*) are given in Hz. The HRMS was recorded in ESI$^+$ mode (70 eV) in Waters mass spectrometer (Model: Xevo-G2QTOF). The absorption and fluorescence spectra were collected using a Shimadzu (Model UV-2450) spectrophotometer and a Hitachi (Model F-7000) spectrofluorimeter, respectively. FTIR spectroscopy was recorded in Spectrum-BX (Perkin Elmer). Solid state PL spectra were recorded in Flurolog Horiba (Model FL-1016, Spectracq). MALDI-TOF study was performed by using Bruker MALDI-TOF-TOF-UltrafleXtreme instrument. Single-Crystal data was collected in low temperature mode using Bruker Apex-II instrument. Morphology and EDX analysis of polymer thin films were carried out by JEOL JSM5800 (Japan) Scanning Electron Microscope with Oxford EDS detector. Molecular weights and polydispersity indices (PDI = M_w/M_n) of polymers were obtained by Gel Permeation Chromatography (GPC) using a Viscotek VE 2001 Triple-Detector Gel Permeation Chromatograph equipped with automatic sampler, pump, injector, inline degasser, column oven (30°C), styrene/divinylbenzene columns with pore sizes of 500 Å and 100,000 Å, VE 3580 refractometer, four-capillary differential viscometer and 90° angle laser and low angle laser (7°) light scattering detector (VE 3210 & VE270). HPLC grade THF was used as the chromatography eluent, at a flow rate of 1.0 mL/min. Samples were dissolved in the eluent (1 mg/ mL) and filtered with a Ministart SRP 15 filter (polytetrafluoroethylene membrane of 0.45 µm pore size) before analysis. Calibration of all three detectors (refractive index, laser light scattering and viscometry) was performed using polystyrene standards (Viscotek). This equipment allows the absolute measurement of homopolymer molecular weights and PDIs. Cyclic voltammetric studies were performed on a BASi Epsilon electrochemical workstation in acetonitrile with 0.1 M tetra-n-butylammoniumhexafluorophosphate ($TBAPF_6$) as the supporting electrolyte at room temperature. The working electrode was a BASi Pt disc electrode, the reference electrode was Ag/AgCl and the auxiliary electrode was a Pt wire. The ferrocene/ferrocenium couple occurs at $E_{1/2}$ = +0.51 (70) V versus Ag/AgCl under the same experimental conditions.

3,3'-bithiophene:

In a 250 mL Schlenk flask 3-Bromothiophene (5 g, 30.6 mmol) was dissolved in 100 mL anhydrous diethyl ether. The solution was cooled to -78°C. To it *n*-BuLi in hexane (1.6 M in hexane, 20 ml, 33 mmol) was added dropwise for 40 min under Ar. The reaction was allowed to stir for 10 min at -78°C and 20 min at -60°C. Then, $CuCl_2$ (4.38 g, 32.5 mmol) was added in one portion at -60°C. The reaction was carefully maintained at -60°C for another 1 h. Then, the reaction mixture was slowly warmed to room temperature and continued stirring for another 18 h at RT. The reaction mixture was quenched by 30 ml water and filtered to remove inorganic impurity. The organic phase was collected and dried over anhydrous $MgSO_4$. Solvent was removed by rotary evaporation. The crude product was purified by silica gel column chromatography using hexane as an eluent to get 1.9 g (76% yield) of 3,3'-bithiophene as white crystalline solid. ^{1}H NMR (200 MHz, $CDCl_3$): δ (ppm) 7.37-7.38 (m, 2H), 7.33-7.36 (m, 4H). ^{13}C{^{1}H} NMR (50 MHz, $CDCl_3$): δ (ppm) 137.4, 126.5, 126.2, 119.9.

Benzo[1,2-b:4,3-b]dithiophene-4,5-quinone (2):

3,3'-Bithiophene (1.5 g, 9 mmol) and 1,2-dichloroethane (DCE) (30 mL) were added to a 250 mL two neck round bottom flask under Ar. Oxalyl chloride (1.4 g, 9 mmol) was added gradually (over 10 min), and the reaction mixture was stirred at 90^{o}C for 4 days. The reaction mixture was then cooled and kept at 0^{o}C for overnight. It was filtered. Product was washed thoroughly by hexane. After drying, the product was obtained as red solid (1.2 g, 64% yield). ^{1}H NMR (400 MHz, $CDCl_3$): δ (ppm) 7.83 (d, 2H, J = 4.8 Hz), 7.29 (d, 2H, J = 4.8 Hz). ^{13}C{^{1}H} NMR (100 MHz, $CDCl_3$): δ (ppm) 174.0, 142.6, 138.6, 135.2, 125.0. FTIR (KBr, cm^{-1}): 1646 ($\nu_{C=O}$, s).

General procedure for synthesis of 3a and 3b:

A mixture of benzaldehyde (2.4 mmol), benzo[1,2-b:4,3-b']dithiophene-4,5-quinone (2.2 mmol), ammonium acetate (72.6 mmol) and acetic acid (20 mL) was heated to 100°C for overnight. The green solution was cooled to room temperature, and 15 mL water was added to stir for 15 min at room temperature. The solution was filtered in a Buchner funnel. The product was washed thoroughly in water and hexane, dried and taken to the next step.

General procedure for synthesis of 4a and 4b:

To an oven dried Schlenk, previously prepared compounds (**3a**/**3b**) (0.8 mmol) in DMF (30 ml) was taken, K_2CO_3 (2.1 mmol) was added and heated to 95°C for 3 h and then cooled to room temperature. To it 1-iodoheptane (0.9 mmol) was added slowly. Reaction mixture was heated to 95°C for overnight. After cooling to room temperature the reaction mixture was poured in 10 mL water. Organic phase was extracted by ethyl acetate via repeated washing in water and dried over anhydrous $MgSO_4$. The solvent was removed under rotary evaporation. Crude product was purified by silica gel column chromatography (Ethyl acetate : Hexane = 10:90) to give solid product (**4a**/**4b**) (50-60% yield).

4a: Brown coloured solid product (0.28 g, 55% yield). ^{1}H NMR (600 MHz, $CDCl_3$): δ (ppm) 7.87-7.78 (dd, 2H, J=5.4 Hz), 7.67 (d, 2H, J = 8 Hz), 7.53-7.48 (dd, 2H, 4.2 Hz), 7.36 (d, 2H, J = 8 Hz), 4.49 (t, 2H, J = 7.8 Hz, 8 Hz), 2.46 (s, 3H), 1.95-1.85 (m, 2H), 1.25-1.21 (m, 8H), 0.87-0.84 (m, 3H) (heptyl proton, 13H). ^{13}C{^{1}H} NMR (150 MHz, $CDCl_3$): δ (ppm) 152.3, 139.9, 132.5, 131.8, 129.6, 127.5, 124.3, 123.2, 122.6, 121.1, 46.5, 31.8, 31.6, 28.8, 26.6, 22.7, 21.6, 14.2.; FTIR (KBr, cm^{-1}): 2918 (ν_{C-H}, stretching, s), 1375 (ν_{C-H}, bending, s); HRMS (ESI$^+$): $C_{25}H_{26}N_2S_2$, Calculated [M+H]$^+$ value (419.1537), experimental 419.1599 [M+H]$^+$ ion peak; λ_{max} (ε, Lmol^{-1}cm^{-1}): 333 nm (1.98 × 10^4), 308 nm (7.1× 10^3).

View Article Online
DOI: 10.1039/C5RA14079J

4b: Brown coloured solid product (0.2 g, 53% yield); ^{1}H NMR (600 MHz, $CDCl_3$): δ (ppm) 7.83 (d, 2H, J = 5.2 Hz), 7.73-7.69 (m, 2H), 7.60 (d, 2H, J = 5.6 Hz), 7.51 (d, 2H, J = 5.2 Hz), 4.59 (t, 2H, J = 6.8 Hz, J = 8 Hz), 1.92-1.84 (m, 2H), 1.27-1.18 (m, 8H), 0.85-0.82 (m, 3H). ^{13}C {^{1}H} NMR (150 MHz, $CDCl_3$): δ (ppm) 150.8, 132.8, 132.2, 131.1, 129.5, 127.7, 124.5, 123.2, 122.6, 121.0, 46.6, 31.7, 31.6, 28.8, 26.6, 22.7, 14.2.; FTIR (KBr, cm^{-1}): 2918 (ν_{C-H}, stretching, s), 1015 (ν_{C-Br}, stretching, s); HRMS: $C_{24}H_{23}BrN_2S_2$, Calculated value (483.4868), experimental 483.3438 (M^+ ion peak); λ_{max} (ε, $Lmol^{-1}cm^{-1}$): 340 nm (1.96×10^4), 270 nm (7.8×10^3).

Synthesis of (4b)$_2$.Cu^{2+}: A clear solution of **4b** (0.2 g, 0.041 mmol) in 5 mL THF was taken into a 50 ml RB flask. 2 mL solution of $Cu(NO_3)_2.6H_2O$ (0.08 g, 0.19 mmol) in MeOH was added. The resulting mixture was stirred for 8 h. The greenish-yellow product was precipitated, filtered off and washed with diethyl ether three times. The brownish colored **4b.**Cu^{2+} was dried in vacuum (yield:76 %).

FTIR (KBr, cm^{-1}): 473 (ν_{Cu-N} w), 1458 ($\nu_{N-O,}$ asymmetric, b), 1261 ($\nu_{N-O,}$ symmetric, b); MALDI-TOF: $C_{48}H_{46}Br_2N_4S_4Cu$, calculated value (1029.520), experimental 1029.700 ([(**4b**)$_2$.Cu(II)]$^+$ molecular ion peak).

General procedure for synthesis of 5a and 5b:

Solution of **4a**/**4b** (1.7 mmol) in THF (10 mL) was taken in 100 mL oven dried Schlenk RB flask. N-bromosuccinamide (3.8 mmol) was added portion wise in 10 min intervals with continuous stirring at room temperature. Completion of the reaction was monitored by TLC. After completion of the reaction the solvent was then removed by evaporation under reduced pressure and the crude product was purified by silica gel column chromatography (hexane as eluent) to give a brown solid of **5a**/**5b** (85-90 % yield).

5a: Yellow solid product (0.85 g, 90% yield). ^{1}H NMR (600 MHz, $CDCl_3$): δ (ppm) 7.72 (s, 1H), 7.65 (s, 1H), 7.62-7.61 (d, 2H, J = 6.0 Hz), 7.36-7.34 (d, 2H, J = 12.0 Hz), 4.40 (t, 2H), 2.48 (s, 3H), 1.90-1.85 (m, 2H), 1.28-1.27 (m, 8H), 0.89-0.87 (m, 3H). ^{13}C{^{1}H} NMR (150 MHz, $CDCl_3$): δ (ppm) 152.9, 140.6, 130.7, 130.3, 130.1, 129.5, 129.4, 127.1, 126.7, 125.6, 125.0, 112.8, 111.7, 46.3, 31.5, 31.3, 29.7, 28.5, 26.3, 22.5, 14.0.

5b: Brown coloured solid (1 g, 88% yield). ^{1}H NMR (600 MHz, $CDCl_3$): δ (ppm) 7.74 (s, 1H), 7.72 (d, 2H, J = 6.0 Hz), 7.67 (s, 1H), 7.65-7.63 (d, 2H, J = 6.0 Hz), 4.39 (t, 2H), 1.90-1.85 (m, 2H), 1.28-1.27 (m, 8H), 0.89-0.87 (m, 3H). ^{13}C{^{1}H} NMR (150 MHz, $CDCl_3$): δ (ppm) 152.0, 134.6, 132.1, 130.9, 130.2, 129.0, 126.8, 125.5, 125.2, 125.0, 124.5, 113.0, 112.1, 46.4, 31.5, 31.4, 28.5, 26.3, 22.5, 14.0.; FTIR (KBr, cm^{-1}): 2918 (ν_{C-H} stretching, s), 1015 ($\nu_{C-Br,}$ b).; HRMS(ESI$^+$): $C_{24}H_{21}Br_3N_2S_2$, Calculated value (641.2789), found 642.8711 $[M+H]^+$.

Synthesis of polymers:

Synthesis Polymer P2:

5b (0.4 g, 0.6 mmol) was dissolved in dry THF (10 mL) and cooled down to -78°C. A solution of *n*-butyllithium in hexanes (1.6 molar *n*-BuLi in hexane, 0.82 mL, 1.32 mmol) was added over a 10 min period and the mixture was stirred for 2 h at -78°C. A solution of tributyltinchloride (0.42 g, 1.3 mmol) in hexane (2 mL) was subsequently added, the mixture was allowed to warm up to room temperature and stirred for 2 h. The solvent was evaporated affording a yellow residue which was used for the next step without further purification. Compound **5b** (0.3 g, 0.5 mmol) was added to the residue and dissolved in 12 mL dry THF. After that the reaction flask was degassed three times by *freeze-pump-thaw* technique. $Pd(PPh_3)_4$ (0.036 gm, 0.003 mmol, 5 mol%) was added to it. The mixture was refluxed for 72 h. The reaction mixture turned chocolate brown from yellow.

Then solvent was concentrated to minimum volume (2 mL) and polymer was precipitated to a stirring hexane. After the complete precipitation hexane was decanted and the polymer was washed another two times with hexane. The polymer was further purified through Soxhlet extraction using hexane, methanol and at last collected in DCM. The DCM part was evaporated to afford the brown colour polymer (0.3 g, 68% yield). ^{1}H NMR (600 MHz, $CDCl_3$): δ (ppm) 7.87-7.61 (m), 4.46-4.34 (m, 2H), 1.92-1.84 (m, 2H), 1.27-1.18 (m, 8H), 0.85-0.82 (m, 3H). ^{13}C{^{1}H} NMR (150 MHz, $CDCl_3$): δ (ppm) 152.3, 139.8, 132.2, 132.0, 131.4, 130.2, 127.7, 124.5, 123.2, 122.6, 120.0, 46.2, 31.9, 31.3, 28.9, 26.3, 22.7, 14.0.; λ_{max} (ε, $Lmol^{-1}cm^{-1}$): 400 nm (1.71×10^4), 279 nm (2.70×10^4). Tetradetector GPC data: M_n = 15,519, M_w = 25,953, PDI = 1.67.

P1 was synthesized following the similar protocol as described for **P2**, starting from **5a** (0.05 g, 0.08 mmol). Yield 0.036 g, 65%. ^{1}H NMR (600 MHz, $CDCl_3$): δ (ppm) 7.66-7.33 (m), 4.51-4.46 (m, 3H), 2.46 (s, 3H), 1.90-1.84 (m, 2H), 1.26-1.15 (m, 8H), 0.81-0.79 (m, 3H).; λ_{max} (ε, $Lmol^{-1}cm^{-1}$): 395 nm(2.26×10^4), 279 nm (2.73×10^4). Tetradetector GPC data: M_n = 14,799, M_w = 26,781, PDI = 1.81.

X-ray data collections and refinement. The yellow colored needle-like single crystals of **4b** suitable for X-ray crystallography, were obtained by layering a THF solution of **4b** on water. Single-crystal X-ray structural studies were performed on a Bruker-APEX-II CCD X-ray diffractometer equipped with an Oxford Instruments low-temperature attachment. Data were collected at 100(2) K using graphite-monochromated Mo K_α radiation (λ_α = R 0.710 73 Å). The frames were indexed, integrated, and scaled using the SMART and SAINT software package,[26] and the data were corrected for absorption using the SADABS program.[27] Pertinent crystallographic data for **4b** is summarized in Table S1†. Two independent molecules of **4b** were located in the asymmetric unit with negligible differences in their metrical parameters. CCDC-1412125 contains the supplementary crystallographic data for this paper. These data can be obtained free of charge from The Cambridge Crystallographic Data Centre via www.ccdc.cam.ac.uk/data_request/cif. The structure was solved and refined using the SHELX suite of programs.[28]All molecular structures were generated by using ORTEP-3 for Windows Version 2.02.[29] The hydrogen atoms were included in geometrically calculated positions in the final stages of the refinement and were refined according to the typical riding model. All non-hydrogen atoms were refined with anisotropic thermal parameters.

View Article Online
DOI: 10.1039/C5RA14079J

References

1. (a) M. Boissinot, H. A. Ho and M. Leclerc, *Angew. Chem. Int. Ed.,* 2002, **41**, 1548; (b) F. Feng, F. He, L. An, S. Wang, Y. Li and D. Zhu, *Adv. Mater.,* 2008, **20**, 2959; (c) G, Harsanyi, *Polymer Films in Sensor Application;* Taylor & Francis Group: Pennsylvania, USA, 1995; (d) Y. Bao, H. Wang, Q. Li, B. Liu, W. Bai, B. Jin and R. Bai, *Macromolecules*, 2012, **45**, 3394; (e) A. Rostami and M. S. Taylor, *Macromol Rapid Commun,* 2012,**33**, 21; (f) S. J. Toal and W. C. Trogler, *J. Mater. Chem.,* 2006, **16**, 2871.
2. For recent reviews and book, see (a) H. N. Kim, W. X. Ren, J. S. Kim and J. Yoon, *Chem. Soc. Rev.,* 2012, **41**, 3210; (b) H. Zhu, J. Fan, B, Wang and X. Peng, *Chem. Soc. Rev.,* 2015, **44**, 4337; (c) R. B. Thompson, *Fluorescence sensors and biosensors;* Taylor & Francis Group: New York, 2006. (d) L. J. Fan, Y, Zhang, C. B. Murphy, S. E. Angell, M. F. L. Parker, B. R. Flynn and W. E. J. Jr., *Coord. Chem. Rev.,* 2009, **253**, 410; (e) X. Feng, L. Liu, S. Wang and D, Zhu, *Chem. Soc. Rev.,* 2010, **39**, 2411.
3. (a) M. Bouachrine, J. P. Lere-Porte, J. J. E. Moreau, F. Sereinspirau and C. Torreilles, *J. Mater. Chem.,* 2000, **10**, 263; (b) J. Pei, X. L. Liu, W. L. Yu, Y. H. Lai, Y. H. Niu and Y. Cao, *Macromolecules*, 2002, **35**, 7274; (c) T. Yasuda, I. Yamaguchi and T. Yamamoto, *Adv. Mater.,* 2003, **15**, 293; (d) M. Kimura, T. Horai, K. Hanabusa and H. Shirai, *Adv. Mater.*, 1998, **10**, 459; (e) Y. Eichen, G. Nakhmanovich, V. Gorelik, O. Epshtein, J. M. Poplawski and E. Ehrenfreund, *J. Am. Chem. Soc.,* 1998, **120**, 10463; (f) M. Zhang, P. Lu, Y. G. Ma and J. C. Shen, *J. Phys. Chem. B,* 2003, **107**, 6535; (g) C. B. Murphy, Y. Zhang, T. Troxler, V. Ferry, J. J. Martin and W. E. Jones, *J. Phys. Chem. B,* 2004, **108**, 1537; (h) C. Xing, Z. Shi, M. Yu and S. Wang, *Polymer,* 2008, **49**, 2698; (i) C. Li, C. Zhou, H. Zheng, X. Yin, Z. Zuo, H. Liu and Y. Li, *J. Polym. Sci., Part A: Polym. Chem.,* 2008, **46**, 1998; (j) T. M. Swager, *Acc. Chem. Res.,* 1998, **31**, 201.
4. (a) F. Tisato, C. Marzano, M. Porchia, M. Pellei and C. Santini, *Medicinal Research Rev*., 2010, **30**, 708; (b) M. C. Linder, *Biochemistry of copper;* Plenum Press: New York, 1991; (c) V. Desai and S. G. Kaler, *Am. J. Clin. Nutr.,* 2008, **88**, 8558; (d) K. G. Daniel, R. H. Harbach, W. C. Guida and Q. P. Dou, *Front. Biosci*, 2004, **9**, 2652; (e) P. C. Bull, G. R. Thomas, M. J. Rommens, J. R. Forbes and W. D. Cox, *Nat. Genet.,* 1993, **5**, 327; (f) B. E. Kim, T. Nevitt and D. Thiele, *J. Nat. Chem. Biol.,* 2008, **4**, 176.
5. (a) K. J. Barnham, C. L. Masters and I. A. Bush, *Nat. Rev. Drug Discovery*., 2004, **3**, 205; (b) R. R. Crichton, D. T. Dexter and J. R. Ward, *Coord. Chem. Rev.,* 2008, **252**, 1189.
6. (a) C. Vulpe, B. Levinson, S. Whitney, S. Packman and J. Gitschier, *Nat. Genet.,* 1993, **3**, 7; (b) S. Lutsenko, A. Gupta, L. J. Burkhead and V. Zuzel, *Arch. Biochem. Biophys.,* 2008, **476**, 22.
7. (a) J. J. Pinto, C. Moreno and M. V. Garcia, *Talanta*, 2004, **64**, 562; (b) N. Pourreza and R. Hoveizavi, *Anal. Chim. Acta.,* 2005, **549**, 124; (c) A. P. S. Gonzales, M. A. Firmino, C. S. Nomura, F. R. P. Rocha, P. V. Oliveira and I. Gaubeur, *Anal. Chim. Acta.,* 2009, **636**, 198; (d) D. Y. Fu and D. Yuan, Spectrochim. Acta. Part *A*, 2007, **66**, 434; (e) A. A. Ensafi, T. Khayamian, A. Benvidi and E. Mirmomtaz, *Anal. Chim. Acta.,* 2006, **561**, 225; (f) Y. Fang, Y. Zhou, Q. Rui and C. Yao, *Organometallics*, 2015, **34**, 2962.
8. (a) A. P. Demchenko, *Introduction to Fluorescence Sensing*; Spinger: USA, 2009; (b) C. Zhang, S. Pu, Z. Sun, C. Fan and G. Liu, *J. Phys. Chem. B.,* 2015, **119**, 4673; (c) K. P. Carter, A. M. Young and A. E. Palmer, *Chem. Rev.,* 2014, **114**, 4564.
9. Representative references regarding fluorescence probe for heavy metal ions (Zn^{2+}, Pb^{2+}, Hg^{2+}, Cd^{2+} and others); see (a) R. Zhou, G. Gao, J. Lan and J. You, *Chem. Commun*., 2011, **47**, 6668; (b) M. Alfonso, A. Tarraga and P. Molina, *Dalton Trans*., 2010, **39**, 8637; (c) M. Alfonso, A. Tarraga, A. Espinosa and P. Molina, *Org. Lett*., 2011, **13**, 2078; (d) M. Alfonso, A. Tarraga and P. Molina, *J. Org. Chem*., 2011, **76**, 939; (e) W. Hong, W. Li, X. Hu, B. Zhao and D. Zhang, *J. Mater. Chem.,* 2011, **21**, 17193; (f) L. N. Neupane, J. M. Kim and C. R. Lohani, *J. Mater. Chem*., 2012, **22**, 4003; (g) J. F. Zhang, S. Kim, J. H. Han, S. J. Lee, Q. Y. Cao, S. J. Lee, T. Pradhan, J. S. Kim and C. Kang, *Org. Lett*., 2011, **13**, 5294; (h) Y. Pang and Y. Xu, *Dalton Trans*., 2011, **40**, 1503; (i) Y. Pang and Y. Xu, *Chem. Commun*., 2010, **46**, 4070; (j) K. Hanaoka, Y. Muramatsu and T. Nagano, *Chem. Eur. J*., 2010, **16**, 568; (k) M. Taki, M. Desaki, Y. Yamamoto, A. Ojida, S. Iyoshi, I. Hamachi, Y. Yamamoto and T. Hirayama, *J. Am. Chem. Soc*., 2008, **130**, 12564; (l) T. Cheng, Y. Xu, S. Zhang, L. Duan and X. Qian, *J. Am. Chem. Soc*., 2008, **130**, 16160; (m) C. Lu, Z. Xu, J. Cui, R. Zhang and X. Qian, *J. Org. Chem. Soc*., 2007, **72**, 3554; For selective sensing of Cu^{2+}; see (n) S. H. Jung, S. P. Kwon, W. J. Lee, I. J. Kim, S. C. Hong, W. J. Kim, S. Yan, Y. J. Lee, H. J. Lee, T. Joo and S. J. Kim, *J. Am. Chem. Soc*., 2009, **131**, 2008; (o) P. Kaur, S. Kaur and S. Singh, *Org. Biomol. Chem*., 2012, **10**, 1497; (p) S. Sarkar and R. Shunmugam, *ACS Appl. Mater. Interfaces,* 2013, **5**, 7379; (q) W. Wang, Q. Wen, Y. Zhang, X. Fei, Y. Li, Q. Yang and X. Xu, *Dalton Trans.,* 2013, **42**, 1827; (r) M. Shellaiah, Y. C. Rajan and H. C. Lin, *J. Mater. Chem.,* 2012, **22**, 8976; (s) M. Shellaiah, Y. H. Wu, A. Singh, M. V. R. Raju and H. C. Lin, *J. Mater. Chem. A,* 2013, **1**, 1310; (t) Y. Chen, C. Zhu, J. Cen, J. Li, W. He, Y. Jiao and Z. Guo, *Chem. Commun.* 2013, **49**, 7632; (u) D. Guo, Z. Dong, C. Luo, W. Zan, S. Yan and X. Yao, *RSC Adv.,* 2014, **4**, 5718; (v) R. Sheng, P. Wang, Y. Gao, Y. Wu, W. Liu, J. Ma, H. Li and S. Wu, *Org. Let.,* 2008, **10**, 5015; (w) S. Goswami, D. Sen and N. K. Das, *Org. Let.,* 2010, **12**, 856.
10. a) S. W. Thomas, G. D. Joly and T. M. Swager, *Chem. Rev.,* 2007, **107**, 1339; (b) J. S. Yang and T. M. Swager, *J. Am. Chem. Soc.,* 1998, **120**, 5321; (c) J. S. Yang and T. M. Swager, *J. Am. Chem. Soc.,* 1998, **120**, 11864; (d) L. X. Chen, W. J. H. Jager, M. P. Niemczyk and M. R. Wasielewski, *J. Phys. Chem. A*, 1999, **103**, 4341; (e) X. Liu and J. Zhu, *J. Phys. Chem. B.*, 2009, **113**, 8214; (f) X. Liu, X, Zhou, X. Shu and J. Zhu, Macromolecules, 2009, **42**, 7634; (g) Q. Zhou and T. M. Swager, *J. Am. Chem. Soc.,* 1995, **117**, 7017; (h) B, Wang and M. R. Wasielewski, *J. Am. Chem. Soc.,* 1997, **119**, 12.
11. (a) R. Satapathy, Y. H. Wu and H. C. Lin, *Org. Lett.*, 2012, **14**, 2564; (b) R. Satapathy, Y. H. Wu and H. C. Lin, *Chem. Comm.,* 2012, **48**, 5668.
12. (a) I. Welterlich and B. Tieke, *Macromolecules*, 2011, **44**, 4194; (b) C. Kaes, A. Katz and M. W. Hosseini, *Chem. Rev., 2000,* ***100***, 3553; (c) T. Yasuda and T. Yamamoto, *Macromolecules*, 2003, **36**, 7513; (d) B. Liu, W. L. Yu, J. Pei, S. Y. Liu, Y. H. Lai and W. Huang, *Macromolecules*, 2001, **34**, 7932.
13. I. Osaka and R. D. Mccullough, *Acc. of Chem. Res.,* 2008, **41**, 1202.
14. (a) L. S. Miguel and A. J. Matzger, *Macromolecules*, 2007, **40**, 9233; (b) E. Bundgaard and F. C. Krebs, *Macromolecules*, 2006, **39**, 2823.
15. (a) Z. Bao, W. K. Chan and L. Yu, *J. Am. Chem. Soc.,* 1995, **117**, 12426; (b) P. M. Beaujuge, W. Pisula, H. N. Tsao, S. Ellinger, K. Mullen and J. R. Reynolds, *J. Am. Chem. Soc*., 2009, **131**, 7514.
16. (a) S. Sirilaksanapong, M. Sukwattanasinitt and P. Rashatasakhon, *Chem. Commun.*, 2012, **48**, 293; (b) J. Hatai, S. Pal and S. Bandyopadhyay, *Tetrahedron Lett.,* 2012, **53**, 4357.
17. (a) S. Cao, Z. Pei, Y. Xu, R. Zhang and Y, Pei, *RSC Adv.*, 2015, **5**, 45888; (b) J. R. Lakowicz, *Principle of Fluorescence*

View Article Online
DOI: 10.1039/C5RA14079J

Spectroscopy, Plenum Publishing Corporation, New York, 2nd Edn, 1991.

18 (a) L. Duan, Y. Xu and X. Qian, *Chem. Commun*., 2008, **44**, 6339; (b) D. Srikun, E. W. Miller, D. W. Domaille and C. J. Chang, *J. Am. Chem. Soc*., 2008, **130**, 4596.

19 (a) Z. Lin, G, Zhang, W, Yang, B, Qiu and G. Chen, *Chem. Commun*., 2012, **48**, 9918; (b) C. Kaewtomg, J. Noiseephum, Y. Uppa, T. Tuntulani and B. Pulpoka, *New J. Chem*., 2010, **34**, 1104; (c) E. A. Albers, S. V. Okreglak and J. C. Chang, *J. Am. Chem. Soc*., 2006, **128**, 9640.

20 (a) X. L. Tang, X. H. Peng, W. Dou, J. Mao, J. R. Zheng, W. W. Qin, W. S. Liu, J. Chang and X. J. Yao, *Org. Let.,* 2008, **10**, 3653; (b) K. M. K. Swamy, S. K. Ko, S. K. Kwon, H. N. Lee, C. Mao, J. M. Kim, K. H. Lee, J. Kim, I. Shin and J. Yoon, *Chem. Commun.,* 2008, 5915.

21 (a) H. S. Jung, P. S. Kwon, J. W. Lee, J. I. Kim, C. S. Hong, J. W. Kim, S. Yan, J. Y. Lee, J. H. Lee, T. Joo and J. S. Kim, *J. Am. Chem. Soc*., 2009, **131**, 2008; (b) C. Xing, M. Yu, S. Wang, Z. Shi, Y. Li and D. Zhu, *Macromol. Rapid Commun*., 2007, **28**, 241.

22 (a) G. D. Santis, L. Fabbrizzi, M. Licchelli, N. Sardona and A. H. Velders, *Chem. Eur, J.* 1996, **2**, 1243; (b) R. Bergonzi, L. Fabbrizzi, M. Licchelli and C. Mangano, *Coord. Chem. Rev.* 1998, **170**, 31.

23 (a) Y. Fu, Q. C. Feng, X. Iang, H. Xu, M. Li and S. Q. Zang, *Dalton Trans.,* 2014, **43**, 5815; (b) M. Li, H. Ge, R. L. Arrowsmith, V. Mirabello, S. W. Botchway, W. Zhu, S. I. Pascu and T. D. James. *Chem. Commun.,* 2014, **50**, 11806.

24 (a) M. Gullotti, L. Casella, A. Pintar and E. Suardi, *J. Chem. Soc. Dalton Trans.,* 1989, **1**, 1979; b) G. Xu, J. Fan and K. Jiao, *Electroanalysis*, 2008, **20**, 1209.

25 D. R. Coulson, L. C. Satek and S. O. Grim, *Inorg. Synth.,* **13**, 121, 1972.

26 SAINT+ Software for CCD Diffractometers; Bruker AXS, Madison, WI, 2000.

27 G. M. Sheldrick, SADABS Program for Correction of Area Detector Data; University of Göttingen, Göttingen, Germany, 1999.

28 (a) SHELXTL Package, version 6.10; Bruker AXS, Madison, WI, 2000. (b) G. M. Sheldrick, SHELXS-86 and SHELXL-97; University of Göttingen, Göttingen, Germany, 1997.

29 L. J. Farrugia, *J. Appl. Crystallogr.,*1997, **30**, 565.

View Article Online
DOI: 10.1039/C5RA14079J

TOC

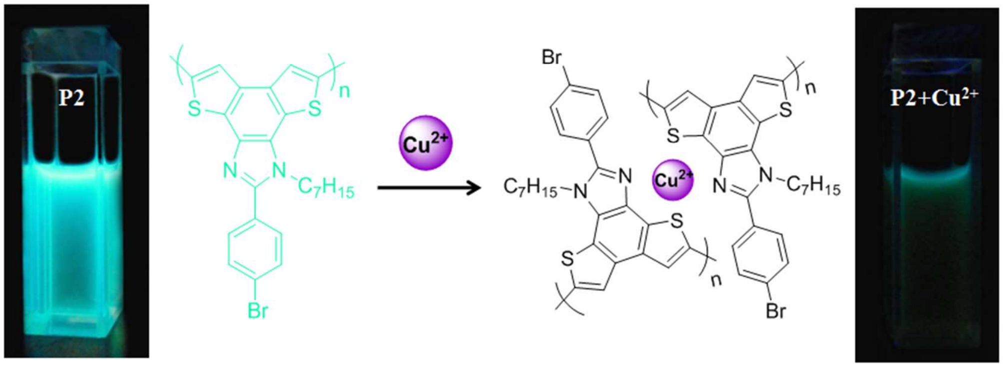

A benzodithieno-imidazole based π-conjugated fluorescent polymer probe showing excellent selectivity towards Cu^{2+} ion through fluorescence quenching.